

# RSC Advances



This is an *Accepted Manuscript*, which has been through the Royal Society of Chemistry peer review process and has been accepted for publication.

*Accepted Manuscripts* are published online shortly after acceptance, before technical editing, formatting and proof reading. Using this free service, authors can make their results available to the community, in citable form, before we publish the edited article. This *Accepted Manuscript* will be replaced by the edited, formatted and paginated article as soon as this is available.

You can find more information about *Accepted Manuscripts* in the [Information for Authors](#).

Please note that technical editing may introduce minor changes to the text and/or graphics, which may alter content. The journal's standard [Terms & Conditions](#) and the [Ethical guidelines](#) still apply. In no event shall the Royal Society of Chemistry be held responsible for any errors or omissions in this *Accepted Manuscript* or any consequences arising from the use of any information it contains.

1 **Micro-aerobic digestion of high-solid anaerobically digested sludge: further**  
2 **stabilization, microbial dynamics and phytotoxicity reduction**

3

4 Xiaowei Li <sup>2,1</sup>, Zonghan Li<sup>1</sup>, Xiaohu Dai<sup>1\*</sup>, Bin Dong<sup>1\*</sup>, Yanfei, Tang<sup>1</sup>

5

6 <sup>1</sup>State Key Laboratory of Pollution Control and Resources Reuse, National  
7 Engineering Research Center for Urban Pollution Control, College of Environmental  
8 Science and Engineering, Tongji University, Shanghai 200092, PR China

9 <sup>2</sup>School of Environmental and Chemical Engineering, Shanghai University,  
10 Shanghai 200444, PR China

11

12 \*Corresponding author. E-mail: lixiaowei419@163.com (Dai X),

13 84370169@qq.com (Dong B)

14 **Abstract**

15       Micro-aerobic digestion was firstly applied for further stabilization and  
16 phytotoxicity reduction of high-solid anaerobically digested sludge (ADS) in room  
17 temperature, mesophilic and thermophilic conditions. Organic matter degradation and  
18 microbial community succession were determined by fluorescent and X-ray  
19 photoelectron spectrometer, and Illumina MiSeq sequencing analysis during the  
20 process. Results showed that specific oxygen uptake rate, volatile solid and ammonia  
21 nitrogen contents of the ADS reduced by 36.1%-86.4%, 8.4%-16.2% and  
22 70.2%-85.4%, respectively after micro-aerobic digestion, and these changes had an  
23 increasing tendency with the temperature. They implied that micro-aerobic digestion  
24 promoted in-depth stabilization of the ADS, which temperature had a positive effect  
25 on. Protein-like and carbohydrate-like groups decreased, and humic acid-like and  
26 carboxyl materials enriched, while microbial community succession shifted from  
27 unassigned bacteria and *Tepidimicrobium* to *Pseudomonas* and Desulfuromonadales  
28 during the micro-aerobic process. Phytotoxicity tests revealed that micro-aerobic  
29 digestion reduced the inhibition of the ADS to germination and root growth of three  
30 plant seeds, but temperature had an adverse impact on the phytotoxicity reduction.  
31 Overall, the findings indicated that mesophilic micro-aerobic digestion was an  
32 alternative technique for the post-treatment of high-solid ADS.

33 **Key words:** sewage sludge; high-solid anaerobically digested sludge; micro-aerobic  
34 digestion; organic matter degradation; phytotoxicity reduction

## 35 1. Introduction

36 Anaerobic digestion is one of the most widely used processes to stabilize sludge  
37 by converting a part of its biodegradable organic matter into biogas, a renewable  
38 energy source <sup>1</sup>. Especially the development of high-solid anaerobic digestion makes  
39 it more economical and efficient <sup>1</sup>. Meanwhile, large amount of anaerobically  
40 digested sludge (ADS) were generated during the process. The ADS had a great  
41 agronomic or land-utilization potential value, due to its high proportion of mineral N  
42 and nutrients <sup>2</sup>. However, the ADS in its basic form may cause poor plant growth and  
43 damage crops because insufficiently-biodegraded organic matter and small-molecule  
44 substances (e.g. ammonia and volatile organic acids) in the ADS will compete for  
45 oxygen or cause phytotoxicity to plants <sup>3, 4</sup>. In addition, unstable ADS would  
46 continue to decompose even after application to soil, in which case, soil microbes  
47 scavenge for the nutrients that should have been made available to plants <sup>4</sup>, causing  
48 the immobilization of the nutrients (e.g. nitrogen) instead of its release for plant  
49 growth. Thus, post-treatment of the ADS was required before it was used for soil  
50 organic amendments or agronomic fertilizer.

51 Recently, micro-aerobic digestion was commended to treat sewage sludge <sup>5, 6</sup>  
52 because of its excellent treatment efficiency and low energy consumption.  
53 Researches showed that the efficiency of H<sub>2</sub>S removal even reached up to 99% in the  
54 micro-aerobic condition <sup>5</sup>, and sufficient micro-aeration could improve the  
55 hydrolysis of carbohydrates and protein <sup>6</sup>. Meanwhile, both of strictly aerobic  
56 bacteria and anaerobes could simultaneously grow in the micro-aerobic system <sup>5</sup>,

57 causing higher VS degradation, compared with a purely anaerobic system.  
58 Micro-aerobic system was only supplied limited oxygen, and thus needed low  
59 energy consumption for aeration. In fact, the micro-aerobic system had many cases.  
60 In one case, it described an anaerobic system into which a trace amount of oxygen is  
61 supplied, while in another it represented an aerobic system with low oxygen supply <sup>5</sup>.  
62 Previous reports focused on an anaerobic system with small amount of oxygen, but  
63 an aerobic system with limited oxygen was paid little attention, because the latter  
64 was liable to cause the accumulation of volatile fatty acids (VFA) <sup>7</sup>. Compared with  
65 raw sludge, the ADS had less biodegradable organic matter, which would relieve the  
66 VFA accumulation. Thus, the micro-aerobic digestion might be a potential and  
67 economic process for post-treatment of the ADS.

68 Previous study about the post-aerobic digestion of the ADS focused on the  
69 treatment performance, e.g. VS reduction and nitrogen removal, and paid little  
70 attention to chemical changes of unstable organic matter in the ADS. Fluorescence  
71 excitation–emission matrix (EEM) spectroscopy was a useful method to investigate  
72 the changing characteristics of fluorescent organic matter in different samples <sup>1,8</sup> and  
73 X-ray photoelectron spectroscopy (XPS) analysis was applied to characterize change  
74 in chemical speciation of organic matter of the samples <sup>9-11</sup>. In the present study, the  
75 two techniques were used to investigate the degradation and transformation  
76 characteristics of organic matters during micro-aerobic digestion of the ADS.

77 Microorganisms in sludge have a close relation to the degradation of unstable  
78 organics and small-molecule phytotoxins. Microbial community succession would

79 occur when the anaerobic environment transfers to the micro-aerobic one. So, it's  
80 significant to explore the changes of microbial population before and after ADS  
81 micro-aerobic digestion. Compared to traditional analytical methods (e.g.  
82 PCR-DGGE technique), next-generation sequencing technology can obtain more  
83 comprehensive and acute data in a shorter analytical time <sup>12</sup>. In the present study,  
84 Illumina MiSeq sequencing technology was applied to characterize the microbial  
85 community succession during the micro-aerobic digestion of the ADS.

86 In spite of undisputable potential resulting from the application of the ADS in  
87 agriculture or landscape, it also involves some threats due to the presence of  
88 pathogens and organic pollutants <sup>13</sup>. The identification of potential threats was  
89 needful to control and reduce the risk involved in the application of the ADS.  
90 Phytotoxicity test could not only evaluate the applicability of the ADS for  
91 agricultural or soil reclamation purposes, but also identify potential threats for the  
92 environment and for human health <sup>13</sup>.

93 The main objectives of this paper were to: (1) investigate treatment  
94 performance of micro-aerobic digestion for the high-solid ADS further stabilization  
95 by chemical parameters and phytotoxicity test; (2) explore possible mechanisms  
96 about the micro-aerobic digestion treating ADS by fluorescence and XPS spectra,  
97 and Illumina MiSeq sequencing techniques; (3) study the effect of temperature on  
98 the micro-aerobic process of the ADS. The study contributes toward development of  
99 a feasible and low-cost process for the ADS post-treatment.

100

## 101 2. Materials and Methods

### 102 2.1. High-solid anaerobically digested sludge

103 The high-solid ADS were collected from a 12 L mesophilic anaerobic digestion  
104 reactor with the sludge retention time (SRT) of 20 days, which had been operated for  
105 60 days and reached the stable state with VS removal rate of  $47.0\% \pm 2.3\%$ . The  
106 anaerobic digestion reactor was operated semi-continuously (once-a-day draw-off and  
107 feeding) and fed with dewatered sludge collecting from Anting WWTP in Shanghai,  
108 China. The characteristics of the ADS were shown as followings: pH,  $7.62 \pm 0.05$ ; total  
109 Alkalinity (TA),  $15822 \pm 754$  mg  $\text{CaCO}_3 \cdot \text{L}^{-1}$ ; total solid content (TS),  $145.2 \pm 2.1$  g·kg<sup>-1</sup>  
110 (wet weight); volatile solid content (VS),  $455.2 \pm 9.3$  g·kg<sup>-1</sup> (dry basis); VFA contents,  
111  $3563 \pm 906$  mg·L<sup>-1</sup>; total kjeldahl nitrogen (TKN),  $8.60 \pm 0.95$  mg N·g<sup>-1</sup>; total  
112 ammonium nitrogen (TAN),  $3.93 \pm 0.26$  mg N·g<sup>-1</sup>.

### 113 2.2. Micro-aerobic digestion experiment

114 Micro-aerobic digestion experiments were carried out in three lab-scale  
115 polyvinyl chloride cylinders, which were designed according to the reference<sup>14</sup>, and  
116 100 mm in inner-diameter, 385 mm in inner-height and 5 mm of thickness, with an  
117 effective volume of about 3 L. Two perforated pipes with 2 mm mesh were installed  
118 at the bottom of each reactor to facilitate aeration. The aeration rate was about 2.4  
119 L·min<sup>-1</sup> to provide a micro-aerobic condition (dissolved oxygen below 0.2 mg·L<sup>-1</sup>)  
120 during the entire experiment<sup>5,6</sup>. An air inlet was installed at the bottom and the outlet  
121 on the top. A vertical stirrer (20 rpm) was fixed in the middle of each reactor for  
122 mixing.

123 The reactors were also operated semi-continuously (once-a-day draw-off and  
124 feeding), and fed with the above ADS. The SRT of the micro-aerobic reactor was 8 d.  
125 At the beginning of experiment, about 800 g of the ADS was fed into each reactor.  
126 The reactors were incubated in room temperature (25 °C), mesophilic (37 °C) and  
127 thermophilic (55 °C) conditions, respectively. Moisture loss was replenished by  
128 adding distilled water to the reactor daily to keep the original volume (subtracting the  
129 volume of sample)<sup>15</sup>.

### 130 **2.3. Sampling and chemical analysis**

131 The influent and effluent sludge (IS and ES) of the micro-aerobic reactors were  
132 periodically sampled for the chemical analysis after the reactors reached the stable  
133 state, in order to evaluate their treatment performances. The experiment ended after  
134 the reactors were operated for 32 days, and the IS and ES samples were collected for  
135 fluorescence EEM, XPS, and microbial community analyses, and phytotoxicity test.

136 pH values were determined by a Mettler Toledo pH meter (Switzerland). Electric  
137 conductivity (EC) values were determined by a Mettler Toledo EC meter  
138 (Switzerland). Specific oxygen uptake rates (SOUR) were determined using about 20  
139 g (wet basis) sludge sample according to the reference<sup>12</sup>. TS contents were estimated  
140 through drying at 105 °C for 24 h, while VS contents were measured through  
141 maintaining the drying sludge at 600 °C for 1 h in a muffle furnace. Dissolved organic  
142 matter (DOC), VFA and TAN contents were determined using the filtrate of the  
143 samples. The filtrate were gained as followings: about 5 g (wet basis) sludge samples  
144 were added 25 ml distilled water, and then mixed on a horizontal shaker at 350 rpm



145 for 15 min; the mixture was centrifuged at 13,000 rpm for 20 min, and then the  
146 supernatant was passed through a 0.45  $\mu\text{m}$  microfiber filter. DOC contents were  
147 determined by a TOC VCPN analyzer (Shimadzu, Japan), and VFA contents were  
148 analyzed by a GC (GC-2010plus, Shimadzu, Japan) with flame ionization detector,  
149 and TAN content were estimated according to the standard methods <sup>16</sup>.

#### 150 **2.4. Organic matter analysis**

151 Fluorescence EEM spectra of the samples were analyzed according to the  
152 reference <sup>17</sup> by a Hitachi F-7000 fluorescence spectrometer (Hitachi High  
153 Technologies, Tokyo, Japan). The filtrate of each sample was gained using the above  
154 method and normalized to a DOC concentration of 10  $\text{mg}\cdot\text{L}^{-1}$ . The emission spectra  
155 were scanned from 290 to 550 nm at 5 nm increments by varying the excitation  
156 wavelength from 250 to 450 nm at 5 nm increments. Surfer 8.0 software was used to  
157 analyze fluorescence spectral data.

158 The freeze-dried and 0.149-mm sieved samples were used for XPS analysis,  
159 which was carried out on a RBD upgraded PHI-5000C ESCA system (Perkin Elmer).  
160 The sample was directly pressed to a self-supported disk (10 $\times$ 10mm) and mounted on  
161 a sample holder, and then transferred into the analyzer chamber. Binding energies  
162 were calibrated by using the containment carbon (C1s = 284.6eV). RBD AugerScan  
163 3.21 software was used for the analysis of the XPS data.

#### 164 **2.5. Microbial community analysis**

165 The DNA of the samples were extracted using a Mo Bio Power Soil<sup>®</sup> DNA  
166 Isolation Kit (Mo Bio laboratories, Inc. Carsbad, CA, USA). The DNA samples were

167 submitted to Shanghai Majorbio Bio-pharm Technology Co.,Ltd (Shanghai, China)  
168 for Illumina MiSeq sequencing analysis. Gene amplicons (16S rRNA) were  
169 conducted using PCR with primers 515F 5'- GTGCCAGCMGCCGCGG)-3' and  
170 907R 5'-CCGTCAATTCMTTTRAGTTT-3'. Each primer was pre-pended with a 8  
171 base barcode sequence and a unique barcode was applied for each sample <sup>18</sup>. The  
172 amplicons were extracted from 2% agarose gels and purified using the AxyPrep  
173 DNA Gel Extraction Kit (Axygen Biosciences, Union City, CA, U.S.). Purified  
174 amplicons were pooled in equimolar and paired-end sequenced (2 × 250) on an  
175 Illumina MiSeq platform according to the standard protocols. The raw reads were  
176 deposited into the NCBI Sequence Read Archive (SRA) database (Accession  
177 Number: SRP067951). Raw fastq files were demultiplexed, quality-filtered using  
178 QIIME (version 1.17) software and reads which could not be assembled were  
179 discarded. Operational taxonomic units (OTUs) were clustered with 97% similarity  
180 cutoff using UPARSE (version 7.1 <http://drive5.com/uparse/>) and chimeric  
181 sequences were identified and removed using UCHIME. The taxonomy of each 16S  
182 rRNA gene sequence was analyzed by RDP Classifier (<http://rdp.cme.msu.edu/>)  
183 against the silva (SSU115) 16S rRNA database using confidence threshold of 70%.

## 184 **2.6. Phytotoxicity assays**

185 Three kinds of ornamental plant seeds, including sunflower (*Helianthus annuus*),  
186 cornflower (*Centaurea cyanus*) and purple morning glory (*Ipomea hederacea*), which  
187 were commended by the OECD for ecotoxicological testing <sup>19</sup>, were used for the  
188 acute and subchronic phytotoxicity assay of the samples.

189 Acute phytotoxicity test (APT) was conducted according to the National  
190 Standard of the People's Republic of China for disposal of sludge from municipal  
191 wastewater treatment (GB/T 23486-2009). In brief, about 10 g of each sample was  
192 dissolved in 30 ml distilled water, and then the mixture was filtrated after shaking at  
193 160 rpm for 60 min. A Petri dish with filter paper was added 5 ml filtrate and 20 seeds,  
194 and then incubated in the dark at 25 °C for 48 h. At the end, the seed germinate rate  
195 and root length of the germinated seed were determined. Each test was repeated five  
196 times. The distilled water was used as control under other similar conditions.

197 Subchronic phytotoxicity test (SPT) was carried out according to OECD  
198 Guidelines<sup>19</sup>. Shortly, growth substrate consisting of inorganic and organic matrices  
199 (volumetric ratio 1:3) was mixed well before adding to the polystyrol seed tray with  
200 20 holes. The inorganic growth substrate consisted of quartz sand, while organic  
201 growth substrate were composed of peat and sludge sample with the ratio of 1:1 (w/w,  
202 dry basis), and 100% peat was served as control. The prepared polystyrol seed trays  
203 were kept in the incubation chamber at 21°C with light/dark regime 16/8 h for 14 d.  
204 Seed germination rate were recorded every days, and root length and fresh weight of  
205 the germinated seeds were determined at the end. The inhibition of the seed  
206 germination for APT and SPT test were estimated with respect to the control  
207 according to the references<sup>4, 13</sup>.

208

### 209 **3. Results and discussion**

#### 210 **3.1. Treatment performance of the micro-aerobic digesters for high-solid ADS**

211 Fig. 1 showed the chemical changes in the IS and ES samples of the three  
212 micro-aerobic digesters. Compared with the IS, The pH of ES increased to  $7.80 \pm 0.06$   
213 at 25 °C, but decreased to  $7.55 \pm 0.10$  and  $7.08 \pm 0.15$  at 37 and 55 °C, respectively (Fig.  
214 1a). The pH value decrease probably resulted from mineralization of ammonia  
215 nitrogen (Fig. 1g), while the pH value increase might be attributed to the loss of  
216 volatile acids (Fig. 1f)<sup>20</sup>. EC values of the ES were significantly lower than that of IS  
217 (Fig. 1b), which might be attributed to loss of soluble salts by leaching and/or  
218 microbial immobilization, and/or to formation of insoluble salts<sup>21</sup>.

219 The ES of the micro-aerobic reactor had lower SOUR and VS content, compared  
220 with the IS. After micro-aerobic digestion, the removal rates of SOUR and VS were  
221 36.1%-86.4% and 8.4%-16.2%, respectively, corresponding to the previous results  
222 from aerobic composting<sup>12</sup>. The results showed that the organic matter of the ADS  
223 was further biodegraded during the process, implying that the micro-aerobic  
224 digestion promoted the bio-stabilization of the ADS. Compared with the results of  
225 raw sewage sludge reported in the previous reference<sup>5</sup>, the VS reduction rates of the  
226 ADS in this study was lower, which might be attributed to the presence of more  
227 biostable organic matter in the ADS<sup>20</sup>.

228 Kumar proposed that there are 4 kinds of VS fractions in sludges: a fraction  
229 degradable only under aerobic conditions, a fraction degradable only under  
230 anaerobic conditions, a fraction degradable under both anaerobic and aerobic  
231 conditions, and a non degradable fraction<sup>22</sup>. The micro-aerobic digestion might  
232 promote the biodegradation of the fraction degradable only under aerobic conditions.

233 Additionally, the removal rates of SOUR and VS gradually increased with  
234 temperature, implying that temperature increase could promote the biodegradation of  
235 the ADS organic matter.

236 Compared with the IS, The ES of micro-aerobic reactor had lower DOC and  
237 VFA contents, which were similar to the changes of the SOUR and VS content,  
238 indicating the degradation of C-containing organic matter and the enhancement of  
239 the ADS stability. Compared with ES of the reactors at 25 and 37 °C (ES-25 and  
240 ES-37), the ES at 55 °C (ES-55) had higher DOC and VFA contents, which was  
241 possibly attributed to higher organic matter hydrolysis rate and limited oxygen  
242 supply in the micro-aerobic condition <sup>5</sup>. Additionally, the TAN removal rates of the  
243 ADS were 70.2%-85.4% after the micro-aerobic digestion, which similar to the  
244 results of the reference <sup>22</sup>, which might be resulted from two pathways, i.e.  
245 nitrification/denitritation and stripping <sup>22</sup>. Fig. S1 of the supplied material (SM)  
246 showed that TAN removal went more through stripping (47%-75%) than through  
247 nitrification/denitritation (25%-53%).

248 In general, after micro-aerobic digestion, the EC, SOUR, VS, DOC, VFA and  
249 TAN contents of high-solid ADS significantly reduced, and the changes had an  
250 increasing tendency as the temperature. These results implied that the micro-aerobic  
251 digestion promoted further stabilization of organic matter in the ADS, which  
252 temperature had a positive effect on.

## 253 **3.2. Degradation and transformation of organic matters**

### 254 **3.2.1. Fluorescence EEM spectra**

255 Fluorescence EEM spectra of the samples from the three aerobic digesters were  
256 shown in Fig. 2. The samples were characterized by several fluorophores, and had  
257 their own excitation/emission wavelength pairs (EEWPs) and specific fluorescence  
258 intensity (Table 1). According to the references <sup>1, 8</sup>, peak 1 and peak 2 belonged to  
259 tyrosine-like and tryptophan-like group (protein-like materials), respectively, while  
260 peak 3 and peak 4 related to the fulvic-like and humic-like acid fractions, respectively.

261 Compared with the IS, the EEM spectra of the ES samples had lower intensity of  
262 peak 1, and higher intensity of peak 3, implying that micro-aerobic digestion  
263 promoted the degradation of protein-like group and the formation of humic-like  
264 substance. Additionally, the spectra of the ES samples had two additional peaks (peak  
265 2 and peak 4), which had longer emission than peak 1 or peak 3 (Fig.S2 of the SM). It  
266 was reported that the peak position emission shifted to longer wavelength with the  
267 increasing content of aromaticity and polycondensation of humic materials <sup>8</sup>. The  
268 results showed that the aromaticity and polycondensation of organic matter in the  
269 ADS increased after the micro-aerobic digestion, implying the formation of more  
270 biostable groups.

271 As the temperature increased, the intensities of the ES samples had a decreasing  
272 tendency in peak 1 and peak 2, and an increasing trend in peak 4. The results showed  
273 that the temperature increase promoted the degradation of protein-like materials, and  
274 the formation of humic acid-like groups. They complemented and confirmed the  
275 above findings that temperature could promote further stabilization of the ADS  
276 organic matter.

### 277 3.2.2. XPS spectra

278 XPS analysis was conducted to determine the chemical characteristics of organic  
279 elements in the sludge samples. Fig. S3 of the SM showed the XPS spectra collected  
280 in the energy range 0-1200 eV of the samples, while Fig. 4 presented representative  
281 peaks of the major elements, C, O and N. According to the previous references<sup>9-11</sup>,  
282 each peak corresponded to different bonds. The C peaks were attributed to four  
283 different bonds: C-C bond of graphite; aliphatic C-H bond in lipids and amino acid  
284 side chains; C singly bound to O or N (C-O, C-N) as in carbohydrates and amines;  
285 and carboxylic carbon with three bonds to oxygen (O-C=O) in carbonyl and  
286 carboxylate. The O peaks were decomposed into three bonds: O=C band in carboxylic  
287 acid, carboxylate, ester, carbonyl and amide; O-C bond, including hydroxide (C-OH);  
288 and acetal and hemiacetal (C-O-C) in polysaccharides. The N peaks were attributed to  
289 three bonds: nitrogen in amine groups (=N-); N-O/C-N bonds in amide or amine; and  
290 N-H bond in ammonia or protonated amine.

291 Table 2 outlined the chemical composition and percentages, in terms of atomic  
292 concentration, of C, O, N, Si, P and S. Compared with the IS, the ES of the  
293 micro-aerobic reactors had lower carbon, C/O and C/N ratios, and higher nitrogen,  
294 oxygen and sulphur. The results showed that the proportion of C-containing materials  
295 decreased, and that of N-, O-, S-containing groups increased after micro-aerobic  
296 digestion, which was possibly resulted from stronger degradation of C-containing  
297 compounds, implying an increase in maturity degree of the ADS<sup>12</sup>. The changes of  
298 the elements had an increasing tendency with temperature, indicating that temperature

299 increase was beneficial to the degradation and transformation of unstable organic  
300 matter in the ADS.

301 After the micro-aerobic digestion, the percentages of C-H, C-(O, N), O-C,  
302 C-O-C and N-H bonds decreased, and that of C-C, O=C-OH, O=C, =N- and N-O/C-N  
303 bonds increased in the ADS, showing that micro-aerobic digestion promoted the  
304 degradation of carbohydrates and amines, and the removal of ammonia, and led to the  
305 enrichment of graphitic carbon, carboxylic acid and nitrocompound. However, the  
306 changes of the groups had no obvious trend with the temperature, which was possibly  
307 resulted from the presence of different functional microbe at different temperature.  
308 The results indicated that the degradation and transformation of these organic matters  
309 were complex and distinctive during the micro-aerobic digestion, and still needed  
310 further study.

311 In sum, XPS analysis showed that the micro-aerobic digestion promoted the  
312 degradation of C-containing materials (e.g. carbohydrates) and amines, and the  
313 enrichment of carboxylic acid and nitrocompound.

### 314 **3.3. Microbial community succession during the aerobic digestion process**

315 Illumina MiSeq Sequencing was used to investigate the change of microbial  
316 community composition before and after micro-aerobic digestion. Each sample  
317 possessed about 10027-15356 quality-filtered reads with the mean length of the  
318 sequences of 428-438 bp (Table S1 of the SM). Fig. S4a of the SM showed the  
319 rarefaction curves at distance cutoff levels of 3%, which indicated reasonable  
320 numbers of sample sequences in this study. Chao and ACE values showed that



321 compared with the IS, the phylotype richness of the ES-55 increased, and that of the  
322 ES-25 and ES-37 decreased (Table S1 of the SM). Shannon diversity index revealed  
323 that compared with the IS, bacterial diversities of ES-25 and ES-37 increased (Fig.  
324 S4b of the SM). The results showed that the micro-aerobic digestion caused a  
325 decrease in bacterial richness of the ADS, and an increase in the diversity, indicating  
326 that microbial community succession occurred during the micro-aerobic digestion  
327 process of the ADS.

328 The sequence tags were assigned into different phylogenetic bacterial taxa using  
329 the RDP classifier and the relative bacterial abundances of the samples on the phylum  
330 level were shown in Fig. 4. The results showed that the samples were dominated by  
331 *Firmicutes* (38.55-88.14%), *Proteobacteria* (2.04-47.89%), *Bacteroidetes*  
332 (2.67-6.09%), *Actinobacteria* (0.80-1.59%) and unclassified bacteria (2.49-41.36%),  
333 with the total abundances of 97.95%-99.74%. Other phylum with little abundance  
334 were also found, including *Thermotogae* (0.00-1.64%), *Synergistetes* (0.07-0.31%),  
335 *Chloroflexi* (0.04-0.21%), *Acidobacteria* (0.02-0.06%) and *Tenericutes* (0.00-0.04%).  
336 After aerobic digestion, the percentage of *Firmicutes* in the ADS decreased, and that  
337 of *Bacteroidetes* and *Proteobacteria* increased. Previous study showed that  
338 *Proteobacteria* were usually found to dominate in activated sludge of WWTP,  
339 followed by *Bacteroidetes* and *Firmicutes*<sup>23</sup>, while *Firmicutes* was the most  
340 dominated phylum in the anaerobic digestion system<sup>24</sup>. Therefore, the results  
341 indicated the microbial community of the ADS had a distinctive succession from the  
342 anaerobic bacteria to aerobic bacteria during the micro-aerobic digestion. As the

343 treatment temperature increased, the percentage of *Bacteroidetes* and *Proteobacteria*  
344 had a decreasing tendency, and *Firmicutes* tended to increase. The results showed that  
345 temperature increase had an adverse on the succession from the anaerobic bacteria to  
346 aerobic bacteria.

347 The top 20 abundant OTU in each sample (a total of 43 OTUs from the four  
348 samples) at 3% cutoff level were selected and compared with the abundances in other  
349 samples. The phylogenetic tree of the 43 OTUs using neighbor-joining analysis was  
350 shown in Fig. 5. For the IS, unassigned bacteria (38.86%) was the most abundant  
351 OTU, followed by two OTUs of *Tepidimicrobium* (14.26% and 9.01%) and  
352 *Proteiniborus* (7.16%). The OTUs were mostly affiliated within *Clostridiales*,  
353 *Firmicutes*, which were well-known obligate anaerobes. Then, three OTUs of  
354 *Pseudomonas* (28.39% in total) were the most abundant OTUs in the ES-25, followed  
355 by unassigned bacteria (8.54%) and *Desulfuromonadales* (6.44%). For the ES-37, the  
356 most abundant OTUs were *Desulfuromonadales* (26.51%), unassigned bacteria  
357 (10.77%) and two OTUs of *Tepidimicrobium* (7.87% and 5.64%). For the ES-55, the  
358 OTUs of *Symbiobacterium* (47.83%) and *Tepidimicrobium* (11.92%) were the most  
359 abundant. Fig. 5 showed that there were considerable changes in the dominate OTUs  
360 composition of the samples after aerobic digestion and with the temperature, which  
361 complemented and confirmed the results at the phylum level.

362 *Pseudomonas* species were universal in the environment and found to be the  
363 dominant bacteria in the mature compost<sup>25</sup>. The Lalucat et al.<sup>26</sup> reported that  
364 *Pseudomonas* strains were capable of denitrification and the degradation of

365 pollutants. Ueda et al.<sup>27</sup> found that *Symbiobacterium* could consume various forms  
366 of organic matter, such as carbohydrate and amino acid, and produce low molecular  
367 weight organic matter, which were well associated with high VS removal rate of the  
368 micro-aerobic reactor at 55 °C. *Desulfuromonadales* was also described as a genera  
369 of sulfate-reducing long-chain fatty acids (LCFA) oxidizers<sup>28</sup>. *Tepidimicrobium* was  
370 described as a thermophilic, peptolytic and strictly nonsaccharolytic bacterium  
371 related to the *clostridia* and grows organotrophically on a number of proteinaceous  
372 substrates<sup>29</sup>, which might be responsible for the degradation of protein-like  
373 materials during the micro-aerobic digestion of ADS. The results indicated that the  
374 microbes such as *Pseudomonas*, *Desulfuromonadales* and *Symbiobacterium*, played  
375 an important part in the degradation and transformation of organic matter during the  
376 micro-aerobic digestion of the ADS.

#### 377 **3.4. Phytotoxicity test**

378 In the preset study, three kinds of ornamental plant seeds, i.e. *Helianthus*  
379 *annuus*, *Centaurea cyanus* L. and *Pharbitis nil* Choisy, were picked for the  
380 phytotoxicity assay of the sludge samples, which was significant to investigate the  
381 effect of the micro-aerobic digestion on the ADS landscape application.

382 Fig. 6 and Fig. S5 of the SM outlined the results of the acute and subchronic  
383 phytotoxicity tests of the IS and ES samples. Both of the acute and subchronic tests  
384 showed that the IS had high inhibition on the germination rate and average root  
385 length of the seeds, corresponding to the previous results that the ADS in basic form  
386 induced the poor plant growth<sup>3, 4</sup>. The inhibition of the ES had a more or less

387 decrease after the micro-aerobic digestion at three temperatures, indicating that the  
388 micro-aerobic digestion reduced the phytotoxicity of the ADS. Additionally, the  
389 inhibition of the ES samples had an increasing tendency as the treatment temperature,  
390 indicating that the temperature had an adverse effect on the reduction of the  
391 inhibition. Therefore, the results showed that micro-aerobic digestion caused a  
392 decrease in the phytotoxicity of the ADS, but treatment temperature increase was not  
393 beneficial for improvement of the ADS land-utilization quality.

394 Previous study showed that the phytotoxicity of sewage sludge was always  
395 attributed to the presence of ammonia, volatile organic acids (VOA), phenolic  
396 compounds, salts and heavy metals<sup>30,31</sup>. Brinton reported that VOA in plant growth  
397 media as low as 300-500 ppm could make a phytotoxic influence on plant seedling,  
398 mainly through the ways of nutrient-ion leakage and root suppression<sup>32</sup>. McLachlan  
399 et al. showed that high soluble salts, which could be reflected by EC value, in the  
400 extracts of digestates may be an important component of phytotoxicity<sup>33</sup>. During  
401 composting process, short-chain volatile fatty acids, primarily acetic acid, was found  
402 to cause the phytotoxic effects of immature compost and the inhibitory effect of  
403 acetic acid on seed germination and root growth was a metabolic phenomenon<sup>34</sup>. In  
404 the present study, Fig. 1 showed that the EC, TAN and VFA contents of the ADS  
405 decreased after micro-aerobic digestion, which might be main factors to cause the  
406 improvement of the ES phytotoxicity. Meanwhile, the ES at 55 °C (ES-55) had  
407 higher VFA contents than the ES at other temperatures, which might be an important  
408 reason for its higher inhibition on the germination of the seeds (Fig. S6 of the SM).

409 Additionally, Himanen et al.<sup>3</sup> found that the phytotoxicity had an increasing trend  
410 with the increase of VFA molecule chain length. Relatively high iso-valeric acid  
411 concentration was also observed in ES-55 (Fig. S6 of the SM), which may be  
412 another reason for the ES-55 possessing the high inhibition.

413

#### 414 **4. Conclusions**

415 Micro-aerobic digestion promoted further stabilization of the high-solid ADS  
416 organic matter, and significant improvement of the seed germination and seedling  
417 growth. The protein-like and polysaccharides-like groups in the ADS reduced, and  
418 the humic acid-like and carboxyl materials had an increasing trend after  
419 micro-aerobic digestion. The microbial community had a distinctive succession from  
420 anaerobic bacteria to aerobic bacteria. However, temperature had a positive effect on  
421 the further stabilization of the ADS and an adverse impact on the microbial  
422 succession and phytotoxicity improvement. In consideration of sludge stabilization,  
423 phytotoxicity reduction and energy consumption, mesophilic micro-aerobic digestion  
424 appears more feasible process for the high-solid ADS post-treatment, compared with  
425 the room-temperature and thermophilic processes.

426

#### 427 **Acknowledgements**

428 The work was financially supported by the National Natural Scientific  
429 Foundation of China (51408423), National Water Pollution Control and Management  
430 Technology Major Projects (2013ZX07315003), National Key Technology Support

431 Program (2014BAC29B01) and Postdoctoral Science Foundation of China  
432 (2015T80452).

433

#### 434 **Appendix A. Supplementary data**

435 One table showing the summary of high-throughput sequencing data of the  
436 samples; one figure showing the contribution of nitrification/denitrification and  
437 stripping ways to TAN reduction; one figure showing the distribution of  
438 excitation-emission maxima; one figure showing the XPS full spectra; one figure  
439 showing the rarefaction and Shannon diversity curves; one figure showing the  
440 inhibition of germination index in APT and fresh weight in SPT; one figure showing  
441 the changes in the VFA contents.

442

#### 443 **References**

- 444 1. X. Li, X. Dai, J. Takahashi, N. Li, J. Jin, L. Dai and B. Dong, *Bioresour. Technol.*, 2014, 159,  
445 412-420.
- 446 2. M. Bustamante, J. Alburquerque, A. Restrepo, C. De la Fuente, C. Paredes, R. Moral and M.  
447 Bernal, *Biomass and bioenergy*, 2012, 43, 26-35.
- 448 3. M. Himanen, P. Prochazka, K. Hänninen and A. Oikari, *Chemosphere*, 2012, 88, 426-431.
- 449 4. G. Ofosu-Budu, J. Hogarh, J. Fobil, A. Quaye, S. Danso and D. Carboo, *Resources,*  
450 *Conservation and Recycling*, 2010, 54, 205-209.
- 451 5. P. Jenicek, J. Koubova, J. Bindzar and J. Zabranska, *Water Sci. Technol.*, 2010, 62, 427-434.
- 452 6. M. Zhu, F. Lü, L.-P. Hao, P.-J. He and L.-M. Shao, *Waste Manage.*, 2009, 29, 2042-2050.
- 453 7. N. Jin, B. Jin, N. Zhu, H. Yuan and J. Ruan, *Bioresour. Technol.*, 2015, 175, 120-127.
- 454 8. X. Li, M. Xing, J. Yang, L. Zhao and X. Dai, *J. Hazard. Mater.*, 2013, 261, 491-499.
- 455 9. H. Liu, G.-Q. Luo, H.-Y. Hu, Q. Zhang, J.-K. Yang and H. Yao, *J. Hazard. Mater.*, 2012, 235,  
456 298-306.
- 457 10. B. Liao, H. Lin, S. Langevin, W. Gao and G. Leppard, *Water Res.*, 2011, 45, 509-520.
- 458 11. L. Hao, S. Liss and B. Liao, *Water Res.*, 2016, 89, 132-141.
- 459 12. X. Li, X. Dai, S. Yuan, N. Li, Z. Liu and J. Jin, *Bioresour. Technol.*, 2015, 175, 245-253.
- 460 13. P. Oleszczuk, A. Malara, I. Joško and A. Lesiuk, *Water Air Soil Poll.*, 2012, 223, 4937-4948.
- 461 14. H. M. Jang, S. K. Park, J. H. Ha and J. M. Park, *Bioresour. Technol.*, 2013, 145, 80-89.

- 462 15. L. Shao, T. Wang, T. Li, F. Lü and P. He, *Bioresour. Technol.*, 2013, 140, 131-137.
- 463 16. APHA, American Public Health Association (APHA), Washington, DC, USA, 21st Edition  
464 edn., 2005.
- 465 17. M. Xing, X. Li, J. Yang, Z. Huang and Y. Lu, *J. Hazard. Mater.*, 2012, 205, 24-31.
- 466 18. L. Ye, M. F. Shao, T. Zhang, A. H. Y. Tong and S. Lok, *Water Research*, 2011, 45,  
467 4390-4398.
- 468 19. OECD, in *OECD Guidelines for the Testing of Chemicals* 2006.
- 469 20. X. Li, X. Dai, L. Dai and Z. Liu, *RSC Advances*, 2015, 5, 82087-82096.
- 470 21. E. Romero, C. Plaza, N. Senesi, R. Nogales and A. Polo, *Geoderma*, 2007, 139, 397-406.
- 471 22. N. Kumar, Master Science, the Virginia Polytechnic Institute and State University, 2006.
- 472 23. T. Zhang, M.-F. Shao and L. Ye, *ISME J.*, 2012, 6, 1137-1147.
- 473 24. C. Sundberg, W. A. Al-Soud, M. Larsson, E. Alm, S. S. Yekta, B. H. Svensson, S. J. Sørensen  
474 and A. Karlsson, *FEMS microbiology ecology*, 2013, 85, 612-626.
- 475 25. M. Danon, I. H. Franke-Whittle, H. Insam, Y. Chen and Y. Hadar, *FEMS Microbiol. Ecol.*,  
476 2008, 65, 133-144.
- 477 26. J. Lalucat, A. Bennasar, R. Bosch, E. García-Valdés and N. J. Palleroni, *Microbiol. Mol. Biol.*  
478 *Rev.*, 2006, 70, 510-547.
- 479 27. K. Ueda, A. Yamashita, J. Ishikawa, M. Shimada, T.-o. Watsuji, K. Morimura, H. Ikeda, M.  
480 Hattori and T. Beppu, *Nucleic Acids Res.*, 2004, 32, 4937-4944.
- 481 28. D. Sousa, M. Pereira, J. Alves, H. Smidt, A. Stams and M. Alves, *Water Sci. Technol.*, 2008,  
482 57, 439-444.
- 483 29. A. Slobodkin, T. Tourova, N. Kostrikina, A. Lysenko, K. German, E. Bonch-Osmolovskaya  
484 and N.-K. Birkeland, *Int. J. Syst. Evol. Microbiol.*, 2006, 56, 369-372.
- 485 30. M. Garcia-Sanchez, I. Garrido, J. Casimiro Ide, P. J. Casero, F. Espinosa, I. Garcia-Romera  
486 and E. Aranda, *Chemosphere*, 2012, 89, 708-716.
- 487 31. M. F. Drennan and T. D. DiStefano, *Bioresour. Technol.*, 2010, 101, 537-544.
- 488 32. W. F. Brinton, *Compost Sci. Util.*, 1998, 6, 75-82.
- 489 33. K. McLachlan, C. Chong, R. Voroney, H. Liu and B. Holbein, Assessing the potential  
490 phytotoxicity of digestates during processing of municipal solid waste by anaerobic digestion:  
491 comparison to aerobic composts, 2002.
- 492 34. A. Shiralipour, D. B. McConnell and W. H. Smith, *Compost Sci. Util.*, 1997, 5, 47-52.

493

494

495 **Figure caption**

496 Fig. 1 chemical changes in the influent and effluent sludge (IS and ES) samples from  
497 three micro-aerobic digesters for further stabilization of anaerobically digested  
498 sludge (ADS) at 25, 37 and 55 °C. (a) pH value; (b) EC, electrical conductivity; (c)  
499 SOUR, specific oxygen uptake rate; (d) VS/TS, the ratio of volatile solid and total  
500 solid contents (dry basis); (e) DOC, dissolved organic carbon; (f) VFA, volatile fatty  
501 acids; (g) TAN, total ammonia nitrogen; (h) TA, total alkalinity.

502 **Fig. 2** Fluorescence excitation–emission matrix spectra of the different sludge  
503 samples. IS, influent sludge; ES-25, ES-37 and ES-55, effluent sludges from the  
504 micro-aerobic digesters operated at 25, 37 and 55 °C, respectively.

505 **Fig. 3** Fitting peaks of C 1s, N 1s and O 1s regions from the XPS spectra of the  
506 sludge samples. IS, influent sludge; ES-25, ES-37 and ES-55, effluent sludges from  
507 the micro-aerobic digesters operated at 25, 37 and 55 °C, respectively.

508 **Fig. 4** Microbial community changes at phylum level during the micro-aerobic  
509 digestion process of anaerobically digested sludge (ADS) revealed by Illumina  
510 MiSeq sequencing. IS, influent sludge; ES-25, ES-37 and ES-55, effluent *sludges*  
511 from the micro-aerobic digesters operated at 25, 37 and 55 °C, respectively.

512 **Fig. 5** Phylogenetic tree (left) and heatmap (right) of top 20 OTUs in each sample at  
513 3% cutoff level. The top 20 abundant OTUs (a total of 43 OTUs for all 4 samples)  
514 were selected and compared with the percentage of their abundance in other samples.  
515 IS, influent sludge; ES-25, ES-37 and ES-55, effluent sludges from the  
516 micro-aerobic digesters operated at 25, 37 and 55 °C, respectively.



517 **Fig. 6** Acute and subchronic phytotoxicity test of the influent and effluent sludge  
518 samples using three types of seeds (*Helianthus annuus*, *Centaurea cyanus* L. and  
519 *Pharbitis nil* Choisy). APT, acute phytotoxicity test; SPT, subchronic phytotoxicity  
520 test; IS, influent sludge; ES-25, ES-37 and ES-55, effluent sludges from the  
521 micro-aerobic digesters operated at 25, 37 and 55 °C, respectively.

522 **Table**

523 Table 1 Ex/Em maxima of fluorescent excitation–emission matrix spectra from the influent  
 524 and effluent sludge samples at 25, 37 and 55 °C (IS, ES-25, ES-37 and ES-55)

Samples	Peak 1		Peak 2		Peak 3		Peak 4	
	Ex/Em <sup>a</sup> (nm)	SFI <sup>b</sup>	Ex/Em (nm)	SFI	Ex/Em (nm)	SFI	Ex/Em (nm)	SFI
IS <sup>c</sup>	275/305	72526	- <sup>d</sup>	-	250/460	16767	-	-
ES-25	275/310	48915	275/340	44261	250/465	22788	330/430	6307
ES-37	275/310	58503	270/410	21638	250/460	25305	345/420	14186
ES-55	275/305	44747	-	-	250/460	22277	330/410	8238

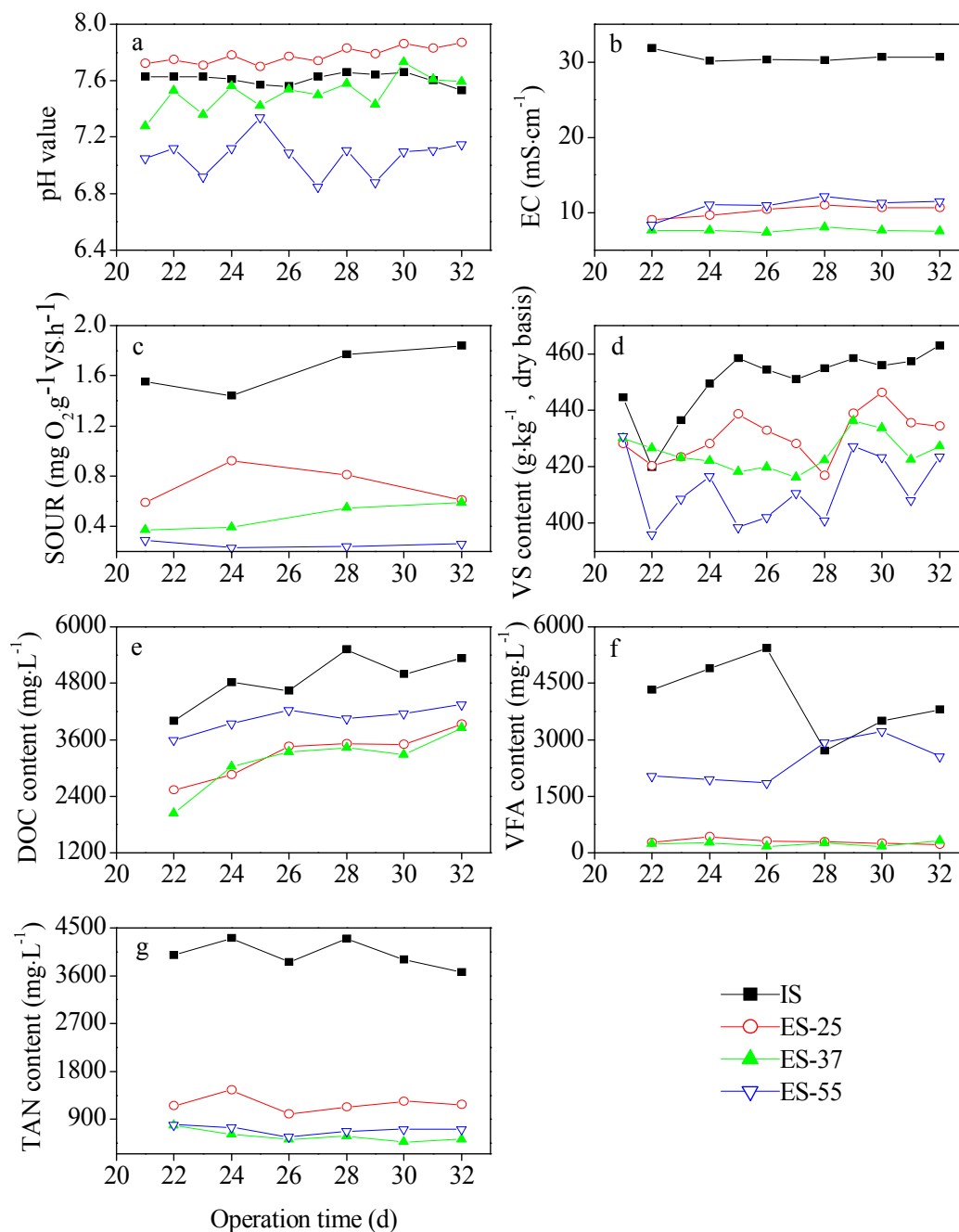
<sup>a</sup>, excitation/emission wavelength pairs ; <sup>b</sup>, specific fluorescence intensity; <sup>c</sup>, influent sludge ; <sup>d</sup>, No data

525 Table 2 Binding energies (eV), assignments and quantitation of XPS spectral bands from the  
 526 influent and effluent sludge samples at 25, 37 and 55 °C (IS, ES-25, ES-37 and ES-55)

Elements	Peak (eV)	IS	ES-25	ES-37	ES-55	Assignments
		Atomic ratios (%)				
Total C	284.6	53.53	50.77	49.47	47.96	- <sup>a</sup>
C1s	283.96±0.25	34	39.9	34.3	48.9	C-C
C1s	284.63±0.09	31.5	15.7	25.2	16.4	C-H
C1s	285.69±0.10	20.4	15.7	13	18.7	C-(O, N)
C1s	287.25±0.60	14.1	28.8	27.5	16	O=C-OH
Total O	532.65±0.10	40.63	42.38	44.11	45.17	-
O1s	531.60±0.20	25.7	45.7	29.4	28.9	O=C
O1s	532.67±0.19	37.1	17.3	34.3	35.7	O-C
O1s	533.79±0.05	37.2	36.9	36.3	35.5	C-O-C
Total N	400±0.16	2.29	3.03	2.66	3.42	-
N1s	398.82±0.26	23.1	25.7	43.8	34.3	=N-
N1s	400.10±0.16	30.1	30.2	32.6	35.7	N-O/C-N
N1s	401.37±0.41	46.9	44.1	23.6	30.1	N-H
Total Si	-	2.41	2.39	2.50	2.09	-
Total P	-	0.76	0.87	0.64	0.69	-
Total S	-	0.38	0.56	0.62	0.67	-
C/O		1.76	1.60	1.50	1.41	
C/N		27.27	19.54	21.70	16.36	

527 <sup>a</sup>, No data

528

529 **Figure**

530

531

532 Fig. 1 chemical changes in the influent and effluent sludge (IS and ES) samples from three

533 micro-aerobic digesters for further stabilization of anaerobically digested sludge (ADS) at 25, 37

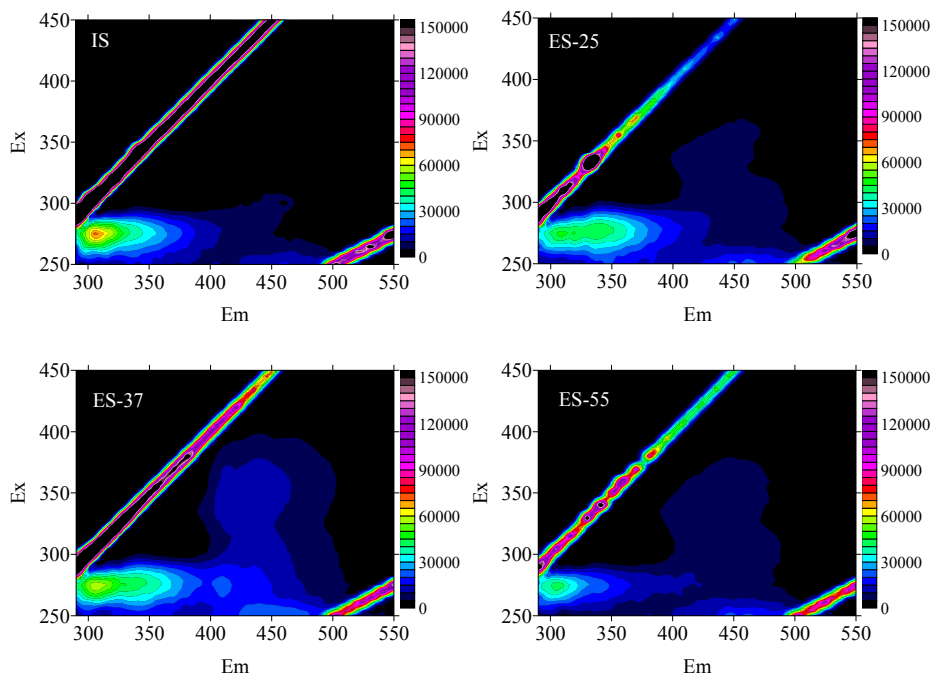
534 and 55 °C. (a) pH value; (b) EC, electrical conductivity; (c) SOUR, specific oxygen uptake rate;

535 (d) VS/TS, the ratio of volatile solid and total solid contents (dry basis); (e) DOC, dissolved

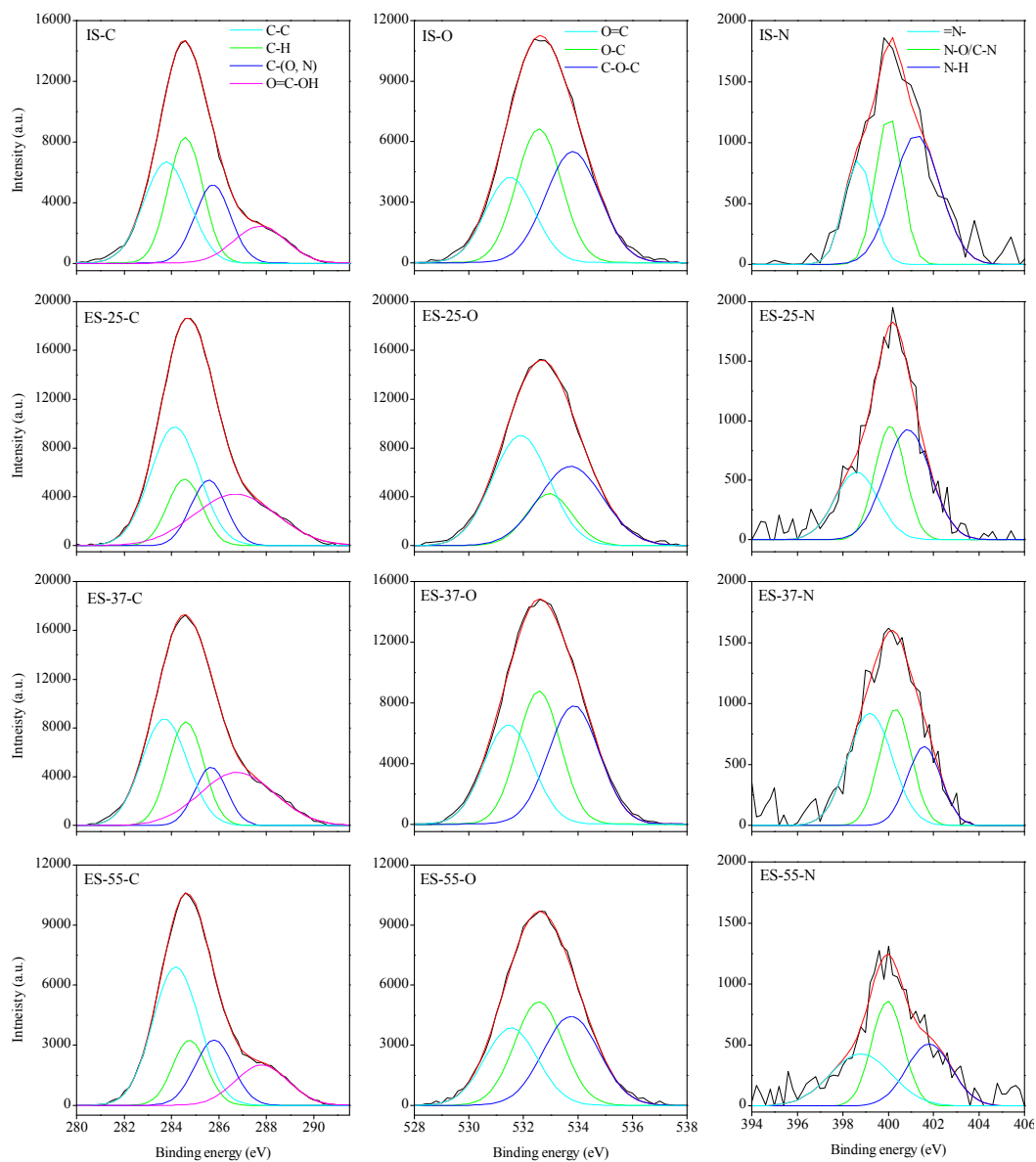
536 organic carbon; (f) VFA, volatile fatty acids; (g) TAN, total ammonia nitrogen; (h) TA, total

537 alkalinity.

538



540 Fig. 2 Fluorescence excitation–emission matrix spectra of the different sludge samples. IS,  
541 influent sludge; ES-25, ES-37 and ES-55, effluent sludges from the micro-aerobic digesters  
542 operated at 25, 37 and 55 °C, respectively.  
543



544

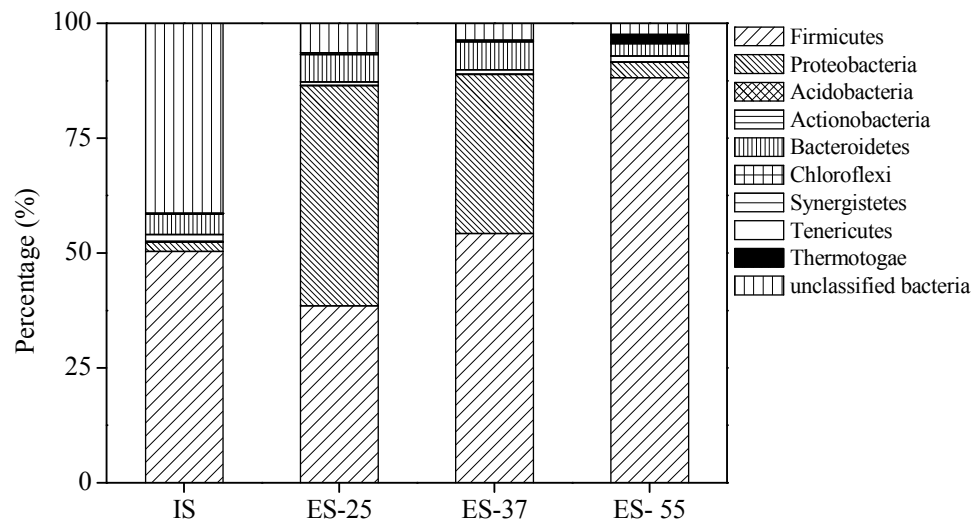
545

546

547

548

Fig. 3 Fitting peaks of C 1s, N 1s and O 1s regions from the XPS spectra of the sludge samples. IS, influent sludge; ES-25, ES-37 and ES-55, effluent sludges from the micro-aerobic digesters operated at 25, 37 and 55 °C, respectively.



549

550

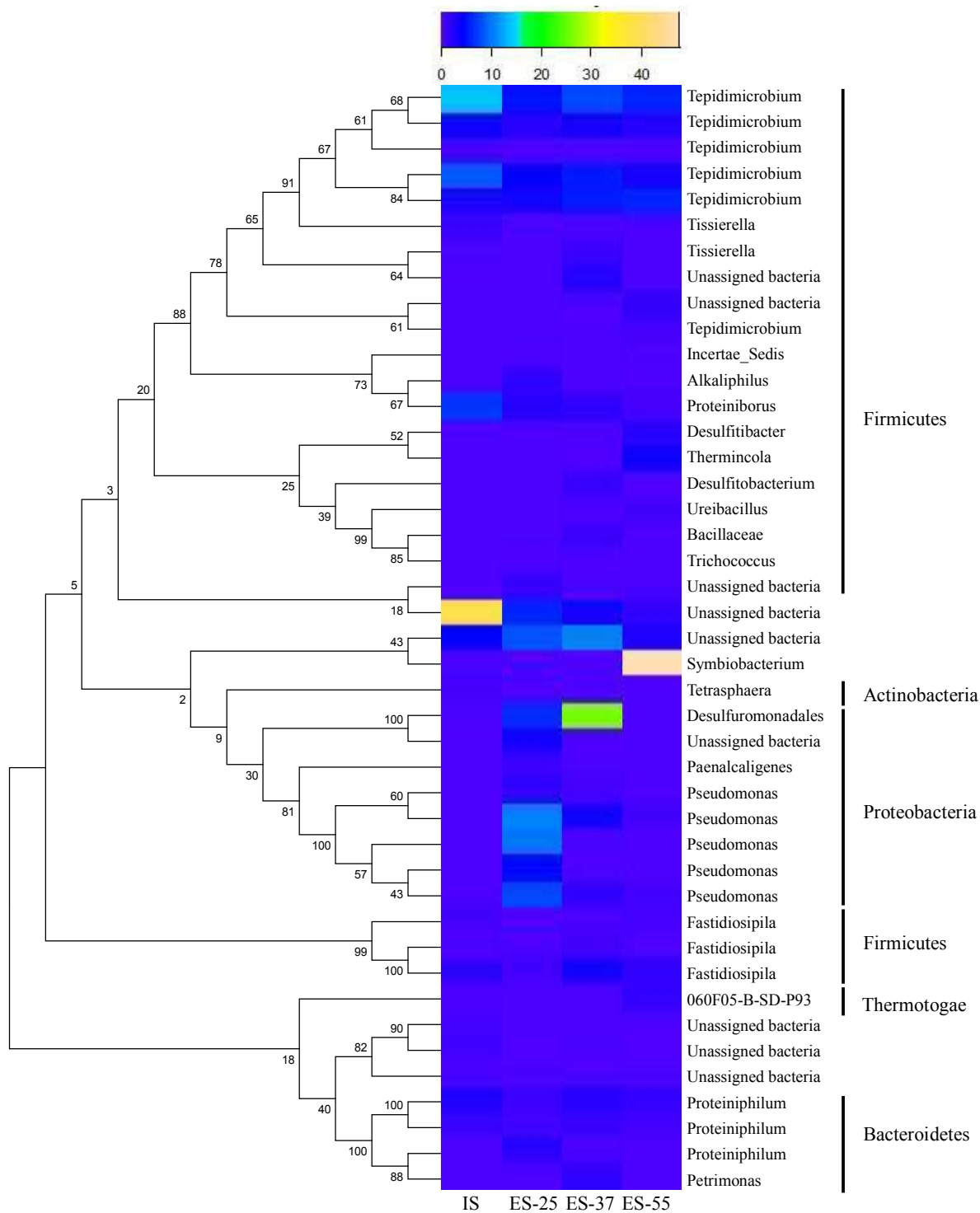
551

552

553

554

Fig. 4 Microbial community changes at phylum level during the micro-aerobic digestion process of anaerobically digested sludge (ADS) revealed by Illumina MiSeq sequencing. IS, influent sludge; ES-25, ES-37 and ES-55, effluent sludges from the micro-aerobic digesters operated at 25, 37 and 55 °C, respectively.

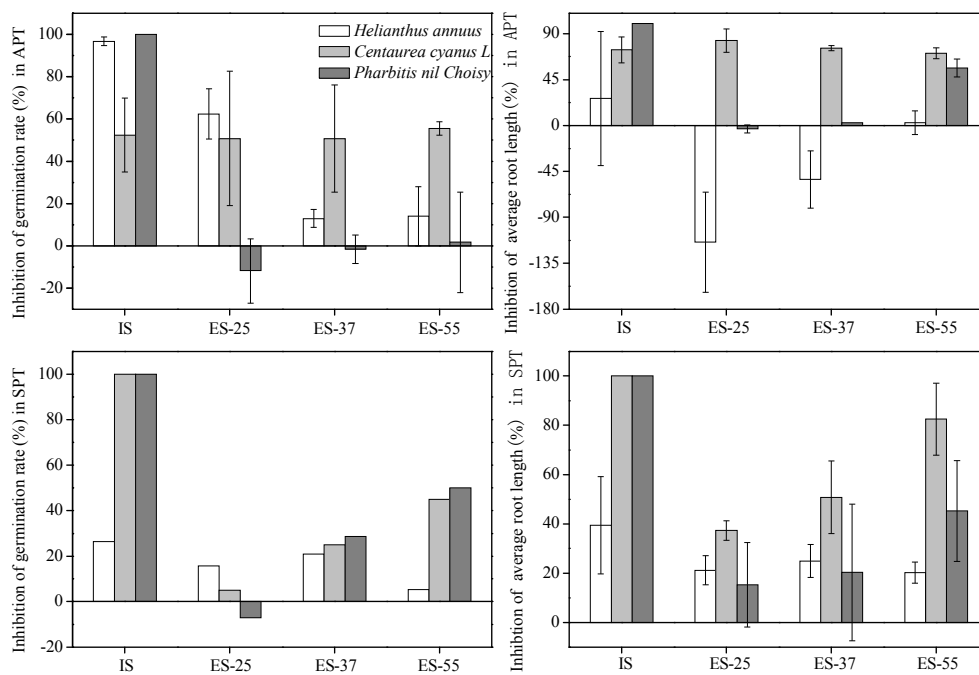


555

556 Fig. 5 Phylogenetic tree (left) and heatmap (right) of top 20 OTUs in each sample at 3% cutoff  
 557 level. The top 20 abundant OTUs (a total of 43 OTUs for all 4 samples) were selected and  
 558 compared with the percentage of their abundance in other samples. IS, influent sludge; ES-25,  
 559 ES-37 and ES-55, effluent sludges from the micro-aerobic digesters operated at 25, 37 and 55 °C,  
 560 respectively.



561



562

563

Fig. 6 Acute and subchronic phytotoxicity test of the influent and effluent sludge samples using three types of seeds (*Helianthus annuus*, *Centaurea cyanus L.* and *Pharbitis nil Choisy*). APT, acute phytotoxicity test; SPT, subchronic phytotoxicity test; IS, influent sludge; ES-25, ES-37 and ES-55, effluent sludges from the micro-aerobic digesters operated at 25, 37 and 55 °C, respectively.

564

565

566

567

568